Conjugation of a Ru(II) arene complex to neomycin or to guanidinoneomycin leads to compounds with differential cytotoxicities and accumulation between cancer and normal cells

Ariadna Grau-Campistany,[a,&] Anna Massaguer,[b,&] Dolors Carrion-Salip,[b] Flavia Barragán,[a,c] Gerard Artigas,[a] Paula López-Senín,[a] Virtudes Moreno[c] and Vicente Marchán*[,a]

[a]*Departament de Química Orgànica and IBUB, Universitat de Barcelona, Barcelona, E-08028, Spain. E-mail: vmarchan@ub.edu.*
[b]*Departament de Biologia, Universitat de Girona, Girona, E-17071, Spain.*
[c]*Departament de Química Inorgànica, Universitat de Barcelona, Barcelona, E-08028, Spain.*

[&]These two authors contributed equally to this work.

ABSTRACT

A straightforward methodology for the synthesis of conjugates between a cytotoxic organometallic ruthenium(II) complex and amino- and guanidinoglycosides, as potential RNA-targeted anticancer compounds, is described. Under microwave irradiation, the imidazole ligand incorporated on the aminoglycoside moiety (neamine or neomycin) was found to replace one triphenylphosphine ligand from the ruthenium precursor $[(\eta^6\text{-}p\text{-cym})RuCl(PPh_3)_2]^+$, allowing the assembly of the target conjugates. The guanidinylated analogue was easily prepared from the neomycin-ruthenium conjugate by reaction with *N,N'*-di-Boc-*N"*-triflylguanidine, a powerful guanidinylating reagent that was compatible with the integrity of the metal complex. All conjugates were purified by semi-preparative HPLC and characterized by ESI and MALDI-TOF MS and NMR spectroscopy. The cytotoxicity of the compounds was tested in MCF-7 (breast) and DU-145 (prostate) human cancer cells, as well as in the normal HEK293 (Human Embryonic Kidney) cell line, revealing a dependence on the nature of the glycoside moiety and the type of cell (cancer or healthy). Indeed, neomycin-ruthenium conjugate (**2**) displayed moderate anti-proliferative activity in both cancer cell lines ($IC_{50} \approx 80$ μM), whereas that of the neamine conjugate (**4**) was inactive ($IC_{50} \approx 200$ μM). However, the guanidinylated analogue of the neomycin-ruthenium conjugate (**3**) required much lower concentrations than the parent conjugate for equal effect (IC_{50} = 7.17 μM in DU-145 and IC_{50} = 11.33 μM in MCF-7). Although the same ranking in anti-proliferative activity was found in the non-tumorigenic cell line (**3** >> **2** > **4**), IC_{50} values indicate that aminoglycoside-containing conjugates are about 2-fold more cytotoxic in normal cells (e.g. IC_{50} = 49.4 μM for **2**) than in cancer cells, whereas an opposite tendency was found with the guanidinylated conjugate, since its cytotoxicity in the normal cell line (IC_{50} = 12.75 μM for **3**) was similar or even lower than that found in MCF-7 and DU-145 cancer cell lines, respectively. Cell uptake studies performed by ICP-MS with conjugates **2** and **3** revealed that guanidinylation of the neomycin moiety had a positive effect on accumulation (about 3-fold higher in DU-145 and 4-fold higher in HEK293), which correlates well with the higher anti-proliferative activity of **3**. Interestingly, despite the slightly higher accumulation in the normal cell than in the cancer cell line (about 1.4-fold), guanidinoneomycin-ruthenium conjugate (**3**) was more cytotoxic to cancer cells (about 1.8-fold), whereas the opposite tendency applied for neomycin-ruthenium conjugate (**2**). Such differences in cytotoxic activity and cellular

accumulation between cancer and normal cells open the way to the creation of more selective, less toxic anticancer metallodrugs by conjugating cytotoxic metal-based complexes such as ruthenium(II) arene derivatives to guanidinoglycosides.

KEYWORDS: ruthenium, cytotoxicity, cellular accumulation, RNA ligands, neomycin, guanidinoneomycin

INTRODUCTION

Organometallic complexes have emerged in recent years as promising anticancer metallodrugs, which could well overcome cisplatin and platinum-related analogues' disadvantages, mainly toxicity and drug resistance in cancer cells.[1-5] Among them, ruthenium(II) complexes bearing a π-bonded arene ligand are particularly interesting since they have shown promising anticancer activities,[6-8] even in cells that had become resistant to cisplatin, such as Sadler's compounds containing *N,N*-chelating ligands.[1,9,10] In addition, some of the Dyson's RAPTA compounds containing pta ligand have shown antimetastatic activity.[11,12] Their so-called "piano-stool" geometry includes an arene unit that stabilizes the ruthenium +2 oxidation state and confers hydrophobicity on the global metal complex, as well as mono- or bidentate ligands, including one or two leaving groups. In most cases, the release of labile chlorido ligands is triggered inside the cell nucleus by the low chloride concentration (4 mM vs ~100 mM in extracellular fluids), allowing for the generation of the activated aqua species that possess the capacity to react with the biological target.[13,14]

Ruthenium offers several advantages over platinum compounds, including reduced toxicity and the possibility of controlling the shape and the chemical and pharmacological properties of the complex by the adequate selection of the arene and the ligands at the "legs" of the "piano-stool" structure.[15,16] Moreover, modification of the non-leaving ligands allows the metal complex to be anchored to a "tumor-targeting device" such as receptor-binding peptides, folic acid or estrogens.[17-24] This targeted strategy has a tremendous potential in the development of more efficient, less toxic, selective metallodrugs in chemotherapy because receptors for these carrier molecules are over-expressed in the membrane of tumoral cells.[25-28]

Another strategy to improve efficiency of a metal-based drug is to increase its affinity with its ultimate biological target. This strategy has been explored mainly with platinum complexes through the covalent attachment to compounds with high affinity for DNA (minor groove binders or intercalators) or to synthetic oligonucleotides or Peptide Nucleic Acids complementary to specific DNA sequences.[29] The cytotoxicity of ruthenium(II) arene complexes, like that of platinum compounds, has been attributed mainly to the binding of their aquation products to DNA.[7,8] However, these complexes' interaction with other potential cellular competitors such as the tripeptide glutathione cannot be ruled out, since they are present in large intracellular concentrations and are

responsible for the detoxification of heavier transition metals.[30] In fact, recent studies have revealed that DNA is not always the primary target for some ruthenium anticancer compounds and that they actually bind more strongly to proteins or enzymes than to DNA.[4,31] Hence, it seems important not only to develop efficient targeting strategies to deliver metallodrugs selectively into cancer cells, but also to direct them towards a particular biological target.

Although, traditionally, metal-based drugs have been designed to target DNA, in therapeutic terms, RNA offers several advantages over DNA as a drug target, since it is involved in many cellular processes, from the regulation of gene expression to protein synthesis.[32-35] In addition, like proteins, RNA adopts complex three-dimensional structures that can be exploited to design specific small molecules to modulate its functions.[36-38] In recent years, microRNAs (miRNAs) have also emerged as new therapeutic targets for cancer therapy since the abnormal expression of these non-coding small RNAs is associated with the pathogenesis of human cancer.[39,40] Like other RNAs, miRNA precursors adopt secondary structures that can be targeted with small molecules, to interfere with miRNA maturation and, for instance, to manipulate miRNA levels.[41,42]

With the aim of developing new metal-based anticancer drugs that could act at the level of RNA, we focused on the conjugation of ruthenium(II) arene complexes with small molecules that had the capacity to recognize selectively RNA over DNA or proteins. Aminoglycoside antibiotics are possibly the most commonly studied RNA ligands,[33,36,43,44] since they have a relatively high affinity with RNA structures and are able to discriminate A-type from B-type duplexes.[43,44] Apart from their selectivity for RNA, aminoglycosides possess several amino functions that are mostly protonated under physiological conditions, which would confer some drug-like properties on the metal complex, such as aqueous solubility. However, aminoglycoside antibiotics are known to have a more inefficient uptake by eukaryotic than by prokaryotic cells.[45] This problem has been solved by replacing their amine functions with guanidinium groups to generate guanidinoglycosides,[46] since these derivatives have higher efficient uptake by eukaryotic cells than their aminoglycoside precursors.[45] In fact, guanidinylated neomycin is known to transport bioactive, high molecular weight cargo into the interior of cells.[47-49] Like naturally occurring aminoglycosides, guanidinoglycosides bind RNA

over DNA preferentially, but they have shown higher binding affinity and selectivity against several RNA targets.[46,50] This strategy was first explored by Tor and collaborators by conjugating a platinum(II) complex with neomycin B and guanidinoneomycin B.[51] The fact that these compounds were able to selectively cross-link an RNA structure derived from HIV Rev Response Element demonstrated that therapeutically relevant RNA structures could be targeted with metal complexes by using the appropriate glycoside.

Herein, we describe for the first time the synthesis, characterization, cellular uptake and antiproliferative activity of conjugates between a ruthenium(II) arene complex, $[(\eta^6\text{-}p\text{-cym})RuCl(Im\text{-}BzCOOMe)(PPh_3)]^+$ (**1**),[24] where Im-BzCOOMe refers to the methyl ester of the 4-(1*H*-imidazol-1-yl)benzoic acid, and neomycin B (**2**), guanidinoneomycin B (**3**) and neamine (**4**) (Scheme 1). In all cases, the metal complex was attached to the amino- or the guanidinoglycoside through the phenyl ring linked to the imidazole ligand. The triphenylphosphine-containing ruthenium(II) complex **1** was recently described as a promising anticancer lead compound, since its anti-proliferative activity is comparable to that of cisplatin in two tumoral cell lines, MCF-7 and DU-145.[24] Interestingly, a direct correlation was found between the cytotoxicity of its octreotide conjugate and the level of expression of the receptors for this peptide in the membrane of tumoral cells.[24]

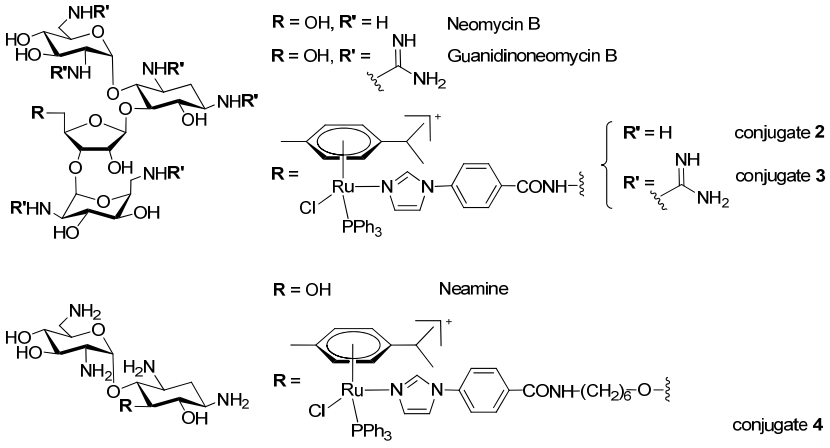

Scheme 1. Structure of the amino(guanidino)glycosides and their ruthenated conjugates.

MATERIALS AND METHODS

General Procedures. Unless otherwise stated, common chemicals and solvents (HPLC grade or reagent grade quality) were purchased from commercial sources and used without further purification. Peptide grade DMF was from Scharlau. Milli-Q water was directly obtained from a Milli-Q system equipped with a 5000-Da ultrafiltration cartridge. Boc-protected amino derivative of neomycin (**5**)[52] and trityl- and *p*-methoxybenzyl-protected amino derivative of neamine (**8**)[53] were prepared as reported elsewhere. Metal complexes $[(\eta^6\text{-}p\text{-cym})RuCl(PPh_3)_2][PF_6]$[54] and $[(\eta^6\text{-}p\text{-cym})RuCl(Im\text{-}BzCOOMe)(PPh_3)][PF_6]$ (**1**)[24] were synthesized according to procedures described elsewhere.

NMR spectra were recorded at 25ºC on a Varian Mercury 400 MHz, Bruker 500 MHz or 600 MHz spectrometer, using deuterated solvents. Tetramethylsilane (TMS) was used as an internal reference (δ 0 ppm) for ^1H spectra recorded in $CDCl_3$ and the residual signal of the solvent (δ 77.16 ppm) for ^{13}C spectra. For CD_3OD, the residual signal of the solvent was used as a reference.

High-Resolution MALDI-TOF mass spectra were recorded on a 4800 Plus MALDI-TOF/TOF spectrometer (Applied Biosystems) in the positive mode, using 2,4-dihydroxybenzoic acid as a matrix. ESI mass spectra (ESI-MS) were recorded on a Micromass ZQ instrument with single quadrupole detector coupled to an HPLC. High-Resolution Electrospray mass spectra (HR ESI MS) were obtained on an Agilent 1100 LC/MS-TOF instrument.

Analytical reversed-phase HPLC analyses were carried out on a GraceSmart RP C_{18} column (250x4 mm, 5 μm, flow rate: 1 mL/min), using linear gradients of 0.045% TFA in H_2O (solvent A) and 0.036% TFA in ACN (solvent B). Large-scale purification was carried out in a Jupiter Proteo semipreparative column (250 x 10 mm, 10 μm, flow rate: 3-4 mL/min), using linear gradients of 0.1% TFA in H_2O (solvent A) and 0.1% TFA in ACN (solvent B). After several runs, pure fractions were combined and lyophilized.

A [Vydac C18]-filled glass column (22x2 cm, 15-20 mm, 300 Å) was used for medium-pressure liquid chromatography (MPLC), using aqueous and ACN solutions containing 0.05% TFA (flow rate: 3 mL/min). Elution was carried out by connecting a piston pump to the mixing chamber of a gradient-forming device and to the top of the glass column. The mixing chamber of the gradient-forming device was the flask containing solvent A, which was connected through a stopcock to the flask containing solvent B. The bottom

of the preparative column was connected to an automatic fraction collector through a UV/Vis detector, which was also connected to a chart recorder using the appropriate ports. The column was equilibrated with 200 mL of solvent A, and 600 mL of each mobile phase was introduced into the appropriate compartments of the gradient-forming device.

Synthesis and characterization of conjugates

Boc-protected imidazole-neomycin derivative 6: 4-(1*H*-Imidazol-1-yl)benzoic acid (233 mg, 1.24 mmol) and PyBOP (643 mg, 1.24 mmol) were suspended in anhydrous DMF (8 mL) under Ar. Upon addition of DIPEA (840 μL, 4.94 mmol), the suspension rapidly dissolved (within 5 min with stirring at rt) and acquired an intense yellow color. This solution was added over the Boc-protected amino derivative of neomycin **5** (300 mg, 0.25 mmol) dissolved in anhydrous DMF (10 mL). Then, the mixture was stirred at rt for 2 h under Ar. After evaporation *in vacuo* the residue was partitioned between AcOEt (100 mL) and H_2O (100 mL). The organic phase was taken up and washed with H_2O (2 x 100 mL) and 10 % aqueous $NaHCO_3$ (2 x 100 mL), dried over anhydrous $MgSO_4$ and filtered, and the solvent was removed *in vacuo*. Purification by silica gel flash-column chromatography (gradient: 0-15 % of MeOH in DCM) afforded the desired product as a white solid (120 mg, 35%). R_f (10% MeOH in DCM): 0.44; HR ESI MS, positive mode: *m/z* 1384.6985 (calcd mass for $C_{63}H_{102}N_9O_{25}$ $[M+H]^+$: 1384.6988); HR MALDI-TOF MS, positive mode: *m/z* 1406.91 (calcd mass for $C_{63}H_{101}N_9NaO_{25}$ $[M+Na]^+$: 1406.6806); ^1H NMR (500 MHz, CD_3OD) δ (ppm): 8.23 (2H, d, *J*=8.5 Hz), 7.93 (1H, s br), 7.79 (3H, d, *J*=8.5 Hz), 7.51 (1H, s br), 5.40 (1H, s br), 5.17 (1H, s), 4.94 (1H, s), 4.32 (1H, m), 4.24 (1H, m), 4.06 (1H, m), 3.96 (1H, m), 3.92 (2H, m), 3.79 (1H, m), 3.75 (2H, m), 3.70 (1H, m), 3.63 (2H, m), 3.55 (3H, m), 3.50 (2H, m), 3.32 (4H, m), 3.16 (1H, m), 1.96 (1H, m), 1.41 (55H, *Boc+1H*, m).

Ruthenium-neomycin conjugate 2: **6** (100 mg, 0.07 mmol) and [(η^6-*p*-cym)$RuCl(PPh_3)_2$][PF_6] (68 mg, 0.07 mmol) were introduced into a microwave reactor. After addition of a 0.4 M LiCl solution in anhydrous DMF (217 μL, 1.2 mol eq LiCl) and triethylamine (103 μL, 10 mol eq), the reaction mixture was diluted with DCM/MeOH 9:1 until a final volume of 10 mL was reached. Microwave irradiation (40 W) was performed at 60ºC under Ar atmosphere for 40 min with continuous magnetic stirring. The reaction mixture was diluted with AcOEt (25 mL) and the organic phase

was washed with H_2O (3 x 25 mL), dried over anhydrous $MgSO_4$ and filtered, and the solvent was removed *in vacuo*.

The crude was treated at 0ºC with a 30% TFA solution in DCM (10 mL) and allowed to come to rt. After 25 min at rt, the solvent was evaporated and the residue was re-dissolved in a 1:1 H_2O/MeOH mixture, lyophilized and purified by MPLC. Pure fractions by analytical HPLC were combined and lyophilized, affording the desired product as the trifluoroacetate-salt of a yellow solid (20.5 mg, 54%).

Characterization: R_t= 14.6 min (analytical gradient: 0 to 100 % in 30 min); HR ESI MS, positive mode: *m/z* 1316.4510 (calcd mass for $C_{61}H_{82}ClN_9O_{13}PRu$ $[M]^+$: 1316.4502), *m/z* 1054.3580 (calcd mass for $C_{43}H_{67}ClN_9O_{13}Ru$ $[M\text{-}PPh_3]^+$: 1054.3590), *m/z* 1018.3827 (calcd mass for $C_{43}H_{66}N_9O_{13}Ru$ $[M\text{-}Cl\text{-}PPh_3\text{-}H]^+$: 1018.3824); HR MALDI-TOF MS, positive mode: *m/z* 1280.4735 (calcd mass for $C_{61}H_{81}N_9O_{13}PRu$ $[M\text{-}Cl\text{-}H]^+$: 1280.47). ^{1}H NMR (500 MHz, CD_3OD) δ (ppm): 8.28 (1H, *Im*, s), 8.05 (2H, *2Ar Ph*, d, *J*=7.5 Hz), 7.53 (2H, *Im*, d, *J*=7.0 Hz), 7.48-7.41 (17H, *2Ar Ph* +15Ar *PPh_3*, d, *m*), 6.12 (1H, Ar *p-cym*, d, *J*=6.0 Hz), 5.94 (1H, Ar *p-cym*, t, *J*=5.5 Hz), 5.87 (1H, *H1´´´*, d, *J*=4.0 Hz), 5.76 (1H, Ar *p-cym*, d, *J*=6.0 Hz), 5.47 (1H, *H1´´*, d, *J*=5.5 Hz), 5.36 (1H, *H1´*, s), 5.17 (1H, Ar *p-cym*, d, *J*=6.0 Hz), 4.57 (1H, *H3´´*, t, *J*=4.5 Hz), 4.37 (1H, *H4´´*, m), 4.31 (1H, *H5´*, m), 4.21 (1H, *H4*, m), 4.15 (1H, *H3´*, m), 4.08-3.97 (5H, *H2´´+H3´´´+H4´´´+H5´´´*+1*H5´´,* m), 3.91 (1H, *H5*, m), 3.69-3.62 (4H, *H2´´´*+1*H5´´+H4´+H6,* m), 3.51 (1H, *H3,* m), 3.44 (1H, *H2´,* m), 3.40-3.35 (2H, 1*H6´*+1*H6´´´,* m), 3.29-3.20 (3H, 1*H6´*+1*H6´´´+H1,* m), 2.52 (1H, *^{i}Pr,* m), 2.45 (1H, 1*H2,* m), 2.08 (1H, 1*H2,* m), 1.77 (3H, *CH_3,* m), 1.20 (3H, *CH_3 ^{i}Pr,* d, *J*=6.5 Hz), 1.17 (3H, *CH_3 ^{i}Pr,* d, *J*=6.5 Hz).

Ruthenium-guanidinoneomycin conjugate 3: The trifluoroacetate salt of conjugate **2** (2 mg, 0.95 μmol) was dissolved in methanol (1 mL) and reacted with *N,N'*-di-Boc-*N''*-triflylguanidine (78 mg, 0.20 mmol) and triethylamine (140 μL, 1 mmol) for 20 days at rt under an Ar atmosphere. After evaporation *in vacuo,* the residue was treated with a 1:1 TFA/DCM mixture and stirred for 4 h at room temperature. The reaction mixture was concentrated under vacuum and, after several co-evaporations from toluene, the crude was dissolved in 0.1% trifluoroacetic acid in water and lyophilized. Purification by analytical HPLC afforded the TFA salt of conjugate **3** as a yellow solid (0.77 mg, 34%).

Characterization: R_t= 17.0 min (analytical gradient: 0 to 100% in 30 min); HR ESI MS, positive mode: *m/z* 784.7942 (calcd mass for $C_{67}H_{95}ClN_{21}O_{13}PRu$ $[M+H]^{2+}$: 784.7946).

^{1}H NMR (600 MHz, D_2O) δ (ppm): 7.93 (1H, s), 7.87 (1H, s), 7.78-7.75 (2H, m), 7.48 (1H, d, *J*=8.4 Hz), 7.33-7.23 (17H, m), 5.97 (1H, Ar *p-cym*, d, *J*=6.0 Hz), 5.68 (1H, *H1´´´*, m), 5.67 (1H, Ar *p-cym*, m), 5.64 (1H, Ar *p-cym*, d, *J*=6.0 Hz), 5.07 (1H, *H1´´*, m), 5.04 (1H, Ar *p-cym*, d, *J*=6.0 Hz), 4.91 (1H, *H1´*, m), 4.30-4.24 (2H, m), 4.01-3.90 (3H, m), 3.70-3.59 (3H, m), 3.54-3.30 (10H, m), 3.26-3.16 (2H, m), 3.05-2.98 (2H, m), 2.30 (1H, *^{i}Pr,* sp, *J*=6.5 Hz), 1.63 (3H, *CH_3,* s), 1.50 (1H, 1*H2,* q, *J*=12 Hz), 1.11 (1H, 1*H2,* t, *J*=7.2 Hz), 0.98 (3H, *CH_3 ^{i}Pr,* d, *J*=6.5 Hz), 0.93 (3H, *CH_3 ^{i}Pr,* d, *J*=6.5 Hz).

(Trt)$_4$(PMB)$_3$-protected imidazole-neamine derivative 9: 4-(1*H*-Imidazol-1-yl)benzoic acid (54 mg, 0.29 mmol) and PyBOP (149 mg, 0.29 mmol) were suspended in anhydrous DMF (1 mL) under Ar. On addition of DIPEA (194 μL, 1.14 mmol), the suspension rapidly dissolved (within 5 min with stirring at rt) and acquired an intense yellow color. This solution was added over the $(Trt)_4(PMB)_3$-protected amino derivative of neamine **8** (100 mg, 0.057 mmol) dissolved in anhydrous DMF (3 mL). Then, the mixture was stirred at rt for 2 h under Ar. After evaporation *in vacuo* the residue was partitioned between AcOEt (10 mL) and H_2O (10 mL). The organic phase was taken up and washed with H_2O (2 x 10 mL), brine (1 x 10 mL) and 10% aqueous $NaHCO_3$ (1 x 10 mL), dried over anhydrous $MgSO_4$ and filtered, and the solvent was removed *in vacuo*. Purification by silica gel flash-column chromatography (gradient: 0-20% of MeOH in DCM) afforded a white solid (33 mg) that corresponds to the desired product. However, **9** was slightly contaminated with tris(pyrrolidin-1-yl)phosphine oxide according to the ^{1}H NMR spectrum (overall yield of **9**: 39.3%). R_f (10% MeOH in DCM): 0.45; HR ESI MS, positive mode: *m/z* 1920.9595 (calcd mass for $C_{128}H_{126}N_7O_{10}$ $[M+H]^+$: 1920.9566), *m/z* 1678.8498 (calcd mass for $C_{109}H_{112}N_7O_{10}$ $[M\text{-}Trt+H]^+$: 1678.8470), *m/z* 1436.7402 (calcd mass for $C_{90}H_{98}N_7O_{10}$ $[M\text{-}2Trt+H]^+$: 1436.7375); ^{1}H NMR (400 MHz, $CDCl_3$) δ (ppm): 7.91 (1H, m), 7.85 (2H, m), 7.68 (6H, m), 7.45 (1H, m), 7.43 (1H, m), 7.38 (9H, m), 7.30 (17H, m), 7.25 (1H, m), 7.23 (2H, m), 7.15 (6H, m), 7.08 (5H, m), 7.00 (12H, m), 6.90 (8H, m), 6.64 (8H, m), 5.30 (1H, s), 4.51 (4H, m), 4.23 (1H, d, *J* = 10.4 Hz), 4.08 (1H, m), 3.78 (3H, s), 3.76 (3H, s), 3.73 (1H, m), 3.69 (3H, s), 3.55 (2H, m), 3.35 (3H, m), 3.06 (1H, s), 2.82 (3H, m), 2.65 (1H, m), 2.55 (1H, m), 2.44 (2H, m), 2.21 (2H, m), 1.48 (5H, m), 1.26 (9H, m). **signals in the spectrum from tris(pyrrolidin-1-yl)phosphine oxide: 3.15 ppm (10H, m) and 1.81 ppm (10H, m).

Ruthenium-neamine conjugate 4: **9** (33 mg, 0.017 mmol) and $[(\eta^6\text{-}p\text{-cym})RuCl(PPh_3)_2][PF_6]$ (24 mg, 0.026 mmol) were dissolved in a 9:1 mixture of

DCM/EtOH (1 mL) in a microwave reactor. After addition of a 0.4 M LiCl solution in anhydrous DMF (78 µL, 1.8 mol eq LiCl) and triethylamine (25 µL, 10 mol eq), the reaction mixture was irradiated (40 W) at 60ºC under Ar atmosphere for 1 h with continuous magnetic stirring. The reaction mixture was diluted with AcOEt (10 mL) and washed with H_2O (3 x 10 mL) and brine (3 x 10 mL), dried over anhydrous $MgSO_4$ and filtered, and evaporated *in vacuo*.

The crude was dissolved in a 1:1 mixture of TFA/anisole (25 mL) under argon. After stirring at rt for 15 h, MeOH (50 mL) was added and evaporated *in vacuo*. The resulting oil was partitioned between DCM (50 mL) and Milli-Q water (50 mL) and the aqueous phase was taken up and washed with DCM (2 x 50 mL) and lyophilized. Purification by semi-preparative HPLC (gradient 0 to 100% in 30 min) afforded the TFA salt of **4** as a yellow solid (13.4 mg, 46%).

Characterization: R_t= 17.5 min (analytical gradient: 0 to 100% in 30 min); HR ESI MS, positive mode: *m/z* 1124.4146 (calcd mass for $C_{56}H_{74}ClN_7O_7PRu$ $[M]^+$: 1124.4119); HR MALDI-TOF MS, positive mode: *m/z* 1090.5 (calcd mass for $C_{56}H_{73}N_7O_7PRu$ $[M\text{-}Cl\text{-}H]^+$: 1088.43). ^{1}H NMR (500 MHz, CD_3OD) δ (ppm): 8.26 (1H, *Ar Im*, m), 7.98 (2H, *2Ar Ph*, d, *J*=9.0 Hz), 7.53 (2H, *Ar Im*, dt, *J*=6.0 Hz, *J'*=1.5 Hz), 7.48-7.39 (17H, *2Ar Ph* +15H Ar PPh_3, m), 6.10 (1H, Ar *p-cym*, dd, *J*=6.0 Hz, *J'*=1.0 Hz), 5.94 (1H, Ar *p-cym*, dd, *J*=6.0 Hz, *J'*=1.5 Hz), 5.84 (1H, *H1´*, d, *J*=3.5 Hz), 5.75 (1H, Ar *p-cym*, dd, *J*=6.0 Hz, *J'*=1.0 Hz), 5.17 (1H, Ar *p-cym*, dt, *J*=6.0 Hz, *J'*=1.5 Hz), 4.14 (1H, *H4*, m), 4.07 (3H, *H5´+H3´*+1*H* *CH₂-NH*, m), 3.76 (1H, *1H* *CH₂-NH*, m), 3.60-3.54 (2H, *H5+H6*, m), 3.49 (1H, *H3*, m), 3.42-3.35 (5H, 1*H6´+H4´+H2´+CH₂-O*, m), 3.26-3.19 (2H, *1H6´+H1*, m), 2.50 (1H, ^{i}*Pr*, qt, *J*=7 Hz), 2.39 (1H, *1H2*, dt, *J*=12 Hz, *J'*=4.0 Hz), 1.99 (1H, *1H2*, q, *J*=12 Hz), 1.76 (3H, CH_3, s), 1.66 (4H, *NH-CH₂-CH₂-CH₂-CH₂-CH₂-*, m), 1.43 (4H, *NH-CH₂-CH₂-CH₂-CH₂-*, m), 1.19 (3H, CH_3 ^{i}*Pr*, d, *J*=7 Hz), 1.16 (3H, CH_3 ^{i}*Pr*, d, *J*=7 Hz).

Cytotoxicity assays in cancer cell lines

The cytotoxicity of the conjugates and of the control compounds was determined by the MTT assay in the breast cancer MCF-7 cell line and the prostate carcinoma DU-145 cell line, as well as in human embryonic kidney 293 (HEK293) non-tumoral cells. Aliquots of 4,000 DU-145, 3,500 MCF-7 and 6,000 HEK293 cells were seeded onto flat-bottomed 96-well plates. 24 h later, the cells were treated for 72 h with the compounds at concentrations ranging from 0 µM to 250 µM. After removal of the treatment, the

cells were washed with PBS and incubated for 3 additional hours with 100 μL of fresh culture medium together with 10 μL of MTT (Sigma-Aldrich). The medium was discarded and DMSO (Sigma-Aldrich) was added to each well to dissolve the purple formazan crystals. Plates were shaken at room temperature for 2 minutes and the absorbance of each well was determined on a Multiscan Plate Reader (ELX800, Biotek, Winooski, USA) at a wavelength of 570 nm. Three replicates were used in each experiment. For each treatment, cell viability was determined as a percentage of the control untreated cells, by dividing the mean absorbance of each treatment by the mean absorbance of the untreated cells. The concentration that reduces cell viability by 50% (IC_{50}) was established for each compound.

Ruthenium accumulation in cancer cells. For ruthenium cell uptake studies, 1.5 x 10^6 DU-145 or HEK293 cells were plated in 100 mm Petri dishes and allowed to attach for 48 h. Next, the plates were exposed to compounds **1-3** at a concentration corresponding to a fifth of their IC_{50} (DU-145: 1.3 μM for **1**, 17 μM for **2** and 1.4 μM for **3**; HEK293: 0.5 μM for **1**, 10 μM for **2** and 2.4 μM for **3**). Additional plates were incubated with medium alone as negative control. After 24 h incubation, the cells were rinsed three times with cold PBS and harvested by trypsinization. The number of cells in each sample was counted manually in a hemocytometer using the Trypan Blue dye-exclusion test. Then the cells were centrifuged to obtain the whole cell pellet for ICP-MS analysis. All experiments were conducted in triplicate.

ICP-MS analysis. The whole cell pellets were dissolved in 400 μL of concentrated 60% v/v nitric acid, and the samples were then transferred into Wheaton v-vials (Sigma-Aldrich) and heated in an oven at 373 K for 18 h. The vials were then allowed to cool, and each cell sample solution was transferred into a volumetric tube and combined with washings with Milli-Q water (1.6 mL). Digested samples were diluted 10 times with Milli-Q to obtain a final HNO_3 concentration of approximately 1.2% v/v. Ruthenium content was analyzed on an ICP-MS Perkin Elmer Elan 6000 series machine at the Centres Científics i Tecnològics of the University of Barcelona. The solvent used for all ICP-MS experiments was Milli-Q water with 1% HNO_3. The ruthenium standard (High-Purity Standards, 1000 μg/mL $\pm$ 5 μg/mL in 2% HCl) was diluted with Milli-Q water to 100 ppb. Ruthenium standards were freshly prepared in Milli-Q water with 1% HNO_3 before each experiment. The concentrations used for the calibration curve were in all

cases 0, 1, 2, 5 and 10 ppb. The isotope detected was ^{101}Ru and readings were made in triplicate. Rhodium was added as an internal standard at a concentration of 10 ppb in all samples.

RESULTS

Synthesis and characterization of ruthenium-amino(guanidino)glycoside conjugates.

Conjugation of the ruthenium complex to neomycin B was planned through the 5''-OH, since this primary hydroxyl group can be regioselectively converted to amino group, allowing the attachment of the imidazole ligand via an amide bond formation. In addition, this modification does not alter the number of chargeable groups that are essential for RNA binding and cell uptake. First, 4-(1H-Imidazol-1-yl)benzoic acid was coupled with the Boc-protected amino derivative of neomycin[52] (**5**, Scheme 2) by using PyBOP as a coupling reagent in anhydrous DMF for 2 h at rt in the presence of DIPEA. The metal complex was assembled on the imidazole-derivatized neomycin (**6**) by reaction with $[(\eta^6\text{-}p\text{-cym})RuCl(PPh_3)_2][PF_6]$ (1 mol equiv) in the presence of LiCl (1.2 mol equiv) and NEt_3 (10 mol equiv) in a DMF/EtOH 9:1 mixture for 40 min at 60ºC under microwave irradiation. Reversed-phase HPLC analysis of the deprotected crude (30% TFA in DCM, 25 min rt) showed the presence of a main peak, which was isolated and characterized by MS as the expected conjugate **2**. Hence, as previously found with imidazole-derivatized peptide-bound resins,[24] the imidazole ligand incorporated in the aminoglycoside moiety is able to replace one of the two PPh_3 ligands in $[(\eta^6\text{-}p\text{-cym})RuCl(PPh_3)_2]^+$. However, in this case it was necessary to use microwave irradiation to assemble the ruthenium complex, since no evidence of the formation of the Boc-protected intermediate **7** was obtained after prolonged heating (24 h) at 50ºC. After purification by reversed-phase medium-pressure liquid chromatography, the trifluoroacetate salt of conjugate **2** was obtained as a yellow solid (overall yield from **6**: 54%) that was unambiguously characterized by mass spectrometry and NMR spectroscopy.

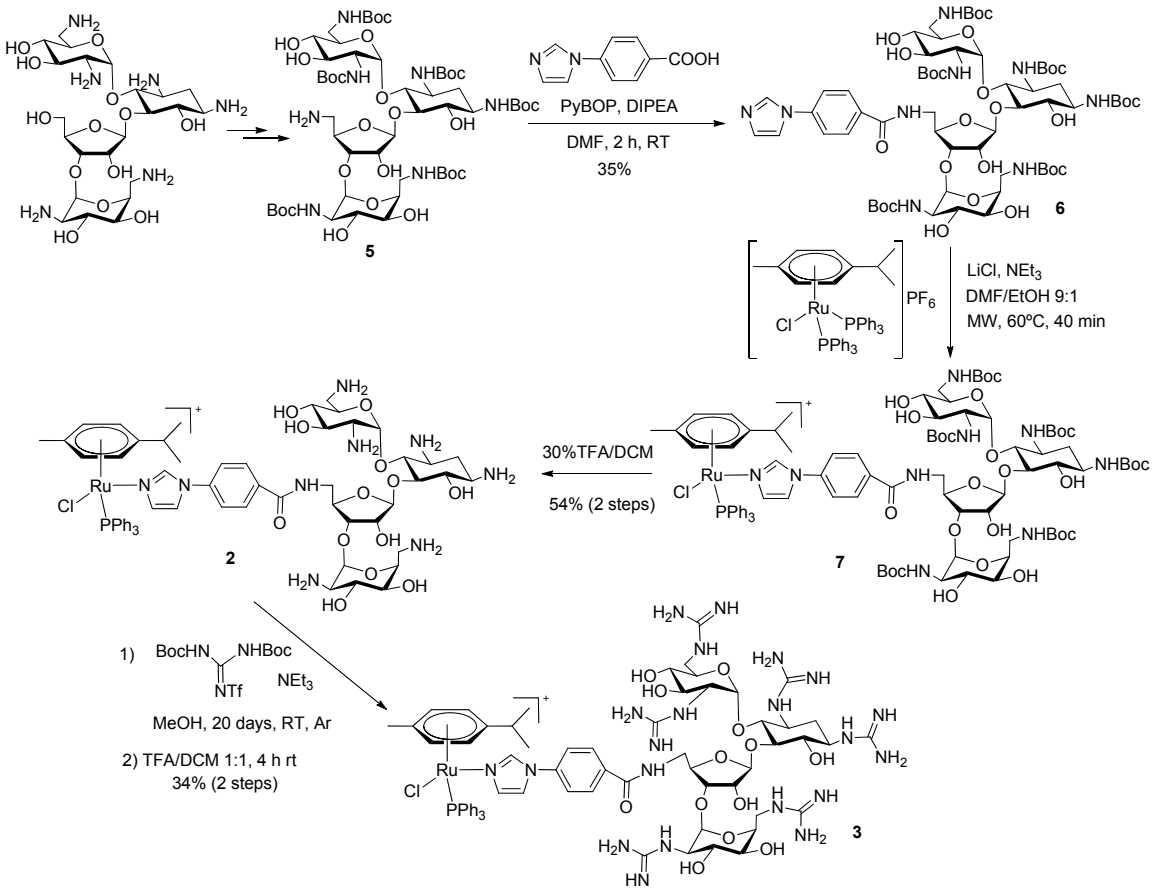

Scheme 2. Synthesis of the ruthenium-neomycin and ruthenium-guanidinoneomycin conjugates.

High-resolution ESI MS analysis of the neomycin-ruthenium conjugate **2** afforded an *m/z* value that was consistent with the calculated value of the monocharged species ($[M]^+$) and with the expected isotopic distribution of ruthenium (Figure 1). In addition, **2** was fully characterized by ^{1}H NMR spectroscopy by using 1D and 2D experiments (COSY and TOCSY). The region of the ^{1}H NMR spectra between 5.0 and 8.5 ppm is shown in Figure 1, where signals from the ruthenium complex (*p*-cymene, imidazole and PPh_3 ligands) and from the aminoglycoside moiety (anomeric H1' protons) are indicated.

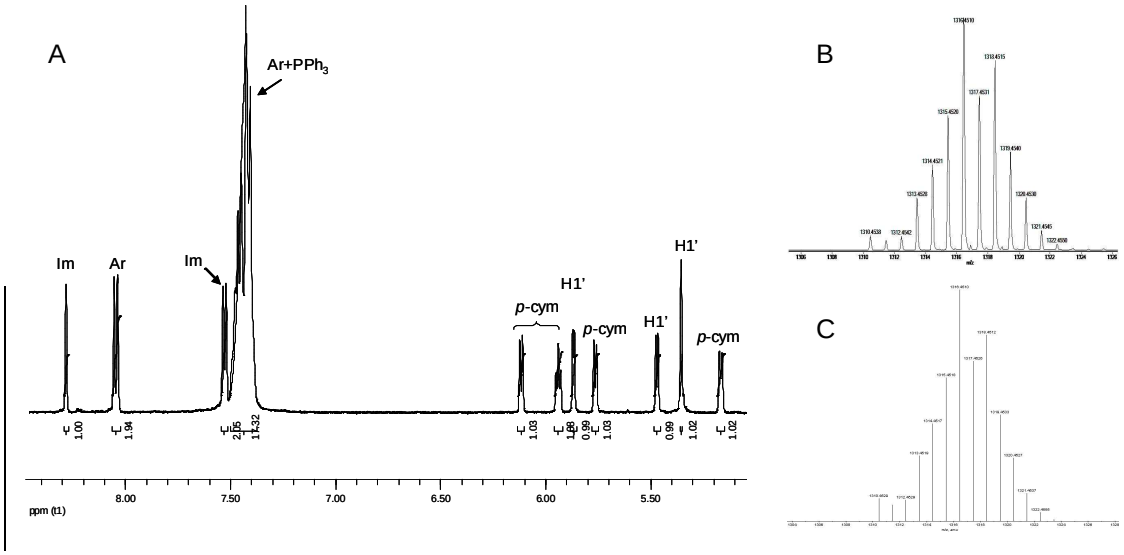

Figure 1. ^{1}H NMR spectra of conjugate **2** (A) in CD_3OD, showing the region between 4.5 and 8.5 ppm. Expanded ESI mass spectrum of the molecular peak of **2** ($[M]^+$), experimental (B) and calculated (C).

Our next objective was the synthesis of the guanidinylated analogue of the neomycin-ruthenium conjugate (compound **3** in Scheme 1), which was planned by using *N,N'*-di-Boc-*N"*-triflylguanidine, a powerful guanidinylating reagent usually employed in the preparation of guanidinoglycosides.[55] Conjugate **2** was dissolved in methanol and reacted with a large excess of *N,N'*-di-Boc-*N"*-triflylguanidine (200 mol equiv) in the presence of triethylamine (1000 mol equiv) at RT under an Ar atmosphere (Scheme 2). The reaction was very slow, especially the incorporation of the sixth guanidinium group, as followed by ESI MS analysis. Once the reaction reached completion (about 20 days), the Boc-protected guanidino conjugate was treated with a TFA/DCM mixture (1:1) for 4 h at RT. Reversed-phase HPLC analysis revealed the presence of a main peak, which was isolated and characterized by high-resolution MS and NMR as the expected conjugate **3** (overall yield from **2**: 34%). It is interesting to note that the ruthenium complex remained unaltered during the prolonged reaction time, which accounts for its high stability in solution (see below).

One of the main problems of aminoglycoside antibiotics is their inherent toxicity, usually nephrotoxicity or ototoxicity, which are associated with non-specific electrostatic binding to RNA.[43,44] To minimize these problems, we selected the pseudodisaccharide known as neamine (Scheme 1), because a reduction in the number

of amino groups in the aminoglycoside scaffold usually gives less toxic compounds. This smaller aminoglycoside is still an attractive starting molecule, since it incorporates rings I and II of most naturally-occurring aminoglycosides, such as neomycin B, which are important structural motifs in the recognition of RNA targets, including rRNA, RRE and TAR RNA. Hence, our next objective was the synthesis of the neamine-ruthenium conjugate (**4**) by the optimized procedure used for the preparation of the neomycin analogue **2**.

The attachment of the metal complex was planned through the 5-hydroxyl group of the 2-deoxystreptamine ring (Scheme 1), since the use of trityl protective groups for the amino functions allows the regioselective protection of all hydroxyl functions with 4-methoxybenzyl groups, except that located at the 5- position.[53] Again, the required imidazole-derivatized neamine (**9**) was obtained by reaction between 4-(1H-Imidazol-1-yl)benzoic acid and the $(Trt)_4(PMB)_3$-protected amino derivative of neamine (**8**) by using PyBOP as a coupling reagent (Scheme 3). The metal complex was assembled on the imidazole ring by reacting **9** with $[(\eta^6\text{-}p\text{-cym})RuCl(PPh_3)_2][PF_6]$ in the presence of LiCl and NEt_3 in a DMF/EtOH 9:1 mixture for 1 h at 60ºC under microwave irradiation. In this case, deprotection was achieved by treatment of the crude with a 1:1 mixture of TFA/anisole under Ar for 15 h at RT. Purification by semi-preparative HPLC afforded the TFA salt of conjugate **4** as a yellow solid (yield from **9**: 46%), which was fully characterized by high-resolution ESI and MALDI-TOF MS and NMR.

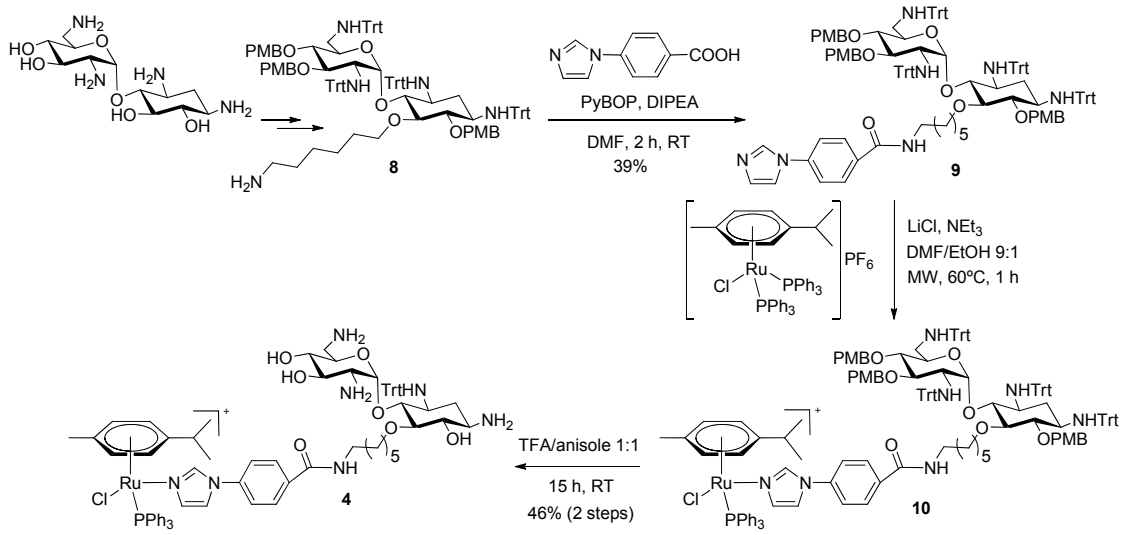

Scheme 3. Synthesis of the ruthenium-neamine conjugate.

Studies on the activation of the ruthenium complex in conjugates 2 and 3

Since the cytotoxic activity of most metallodrugs is intimately related to their hydrolysis behavior in aqueous media, prior to cytotoxicity studies we wanted to assess whether hydrolysis of the Ru-Cl bond occurs when the ruthenium complex is conjugated to the glycoside carrier. This process is known to facilitate the interaction of the metal with the biological target (e.g. nucleic acids or proteins) through the generation of monofunctional adducts on guanine nucleobases by the activated aqua species. Although anticancer activity of ruthenium(II) arene complexes has been attributed in most cases to DNA ruthenation, some compounds such as **1** do not experience aqueous hydrolysis of the Ru-Cl bond,[24] which hinders the covalent interaction with the biological target.

On the basis of these precedents, the stability of conjugates **2** and **3** (Scheme 1) was investigated in aqueous solution at a chloride concentration mimicking the typical cell nucleus (4 mM). As previously found with **1** or its peptide conjugate,[24] reversed-phase HPLC analysis together with MS revealed that no hydrolysis occurred in the case of the ruthenium-(guanidino)neomycin conjugates on incubation at 37ºC for 48 h. Surprisingly, the compounds also remained unaltered upon incubation at 37ºC for 72 h with a large excess of glutathione (250 mol equiv) under physiologically relevant conditions (pH 7 phosphate buffer containing 22 mM NaCl, the cytoplasmatic concentration of chloride).[30] These results suggest that the ruthenium moiety in the amino(guanidino)glycoside conjugates (**2**-**4**) does not follow the typical activation mechanisms of most organometallic anticancer complexes (e.g. hydrolysis of the Ru-Cl bond and/or redox activation through the participation of the tripeptide glutathione).[14] The presence of a bulky ligand such as triphenylphosphine might explain this behavior, which is different from other anticancer ruthenium(II) arene complexes such as [(η^6-biphenyl)Ru(en)Cl)]$^+$.[1,14]

Cytotoxicity in cancer (MCF-7 and DU-145) and normal (HEK293) cell lines

Our next objective was to evaluate the cytotoxicity of conjugates **2**, **3** and **4** to determine their potential as anticancer agents. Their anti-proliferative activity, together with that of cisplatin as positive control and the unconjugated compounds (complex **1**, neomycin, neamine and guanidinoneomycin), was first determined in two human tumor cell lines, the breast cancer cell line MCF-7 and the prostate carcinoma cell line DU-145, by using the MTT test that measures mitochondrial dehydrogenase activity as an

indication of cell viability (Table 1). The compounds were screened at a wide range of concentrations (from 0 to 250 μM) to determine the concentration that inhibits cell growth by 50% (IC_{50}). The compounds that did not inhibit cell growth by more than 50% at 250 μM were considered to be inactive. Interestingly, conjugates **2-4** were completely soluble in water.

	IC_{50} (μM)/cell lines		
Compound	MCF-7	DU-145	HEK293
Cisplatin	3.04 ± 0.25	3.10 ± 0.00	4.63 ± 1.60
Ruthenium complex **1**	3.99 ± 1.45	6.48 ± 0.54	2.50 ± 0.71
Ru-neomycin conjugate **2**	84.67 ± 5.13	84.63 ± 15.87	49.40 ± 17.25
Ru-neamine conjugate **4**	200.75 ± 15.75	221.67 ± 3.33	125.00 ± 2.02
Neomycin or neamine	> 250	> 250	> 250
Ru-guanidinoneomycin conjugate **3**	11.33 ± 2.56	7.17 ± 0.29	12.75 ± 1.32
Guanidinoneomycin	> 250	> 250	> 250

Table 1. Sensitivity of tumor MCF-7 and DU-145 cells and of non-tumorigenic HEK293 cells to cisplatin, compounds **1-4** and control amino(guanidino)glycosides. The concentration of the compounds that inhibits cells viability by 50% **(**IC_{50}) after 72 h was determined by means of the MTT assay. Each value represents the mean of three independent experiments ± standard error.

The concentration-response curves, plotted in Figure 2, revealed that the cytotoxic activity of conjugates **2-4** was very dependent on the nature of the glycoside moiety in these cell lines. As previously reported,[24] the effectivity of the complex $[(\eta^6\text{-}p\text{-cym})RuCl(Im\text{-}BzCOOMe)(PPh_3)]^+$ (**1**) was comparable to that of cisplatin and slightly higher in MCF-7 cells than in DU-145 cells, showing IC_{50} values of 3.99 ± 1.45 μM and 6.48 ± 0.54 μM, respectively (Table 1). Neomycin-ruthenium conjugate **2** had moderate anti-proliferative activity in both cell lines (IC_{50}≈ 80), but its guanidinylated analogue (**3**) was highly cytotoxic (IC_{50}= 11.33 ± 2.56 in MCF-7 cells and IC_{50}= 7.17 ± 0.29 in DU-145 cells), with an IC_{50} value similar to that of complex **1** in the prostate cancer cell line. However, conjugation of the ruthenium complex to the small neamine aminoglycoside led to a strong decrease in cytotoxic activity (IC_{50}≈ 200). Interestingly,

neither the aminoglycosides alone (neomycin or neamine) nor guanidinoneomycin were found to be cytotoxic (IC_{50} > 250).

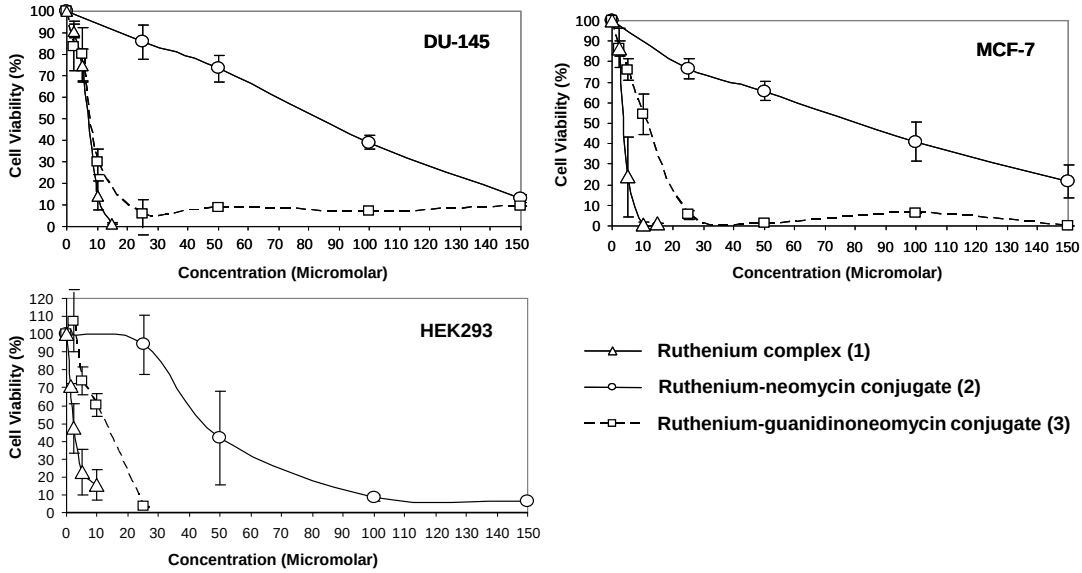

Figure 2. Cytotoxic effect of compounds **1-3** in the DU-145, MCF-7 and HEK293 cell lines. Cells were treated for 72 h with the indicated concentrations of each compound. Cell viability was determined by the MTT assay. Each point in the graphs represents the mean of three independent experiments ± SD.

Despite the promising anticancer activities of the ruthenium-glycoside conjugates, particularly those of guanidinoneomycin conjugate **3**, an efficient targeted strategy requires that the potential anticancer drug must be less toxic to normal cells than to tumor cells. Otherwise, such anticancer agents generate undesired side-effects, as current platinum drugs in clinical use do.

To assess the conjugates' selectivity for tumor cells rather than normal cells, we determined the cell viability of a non-tumorigenic HEK293 cell line, in the presence of conjugates **2-4**. To our surprise, ruthenium complex **1** (IC_{50}= 2.50 μM) was found more cytotoxic in the normal cell line than in the two cancer cell lines, whereas cisplatin cytotoxicity was similar (IC_{50}= 4.63 μM) (Table 1). Again, control aminoglycosides and guanidinoneomycin were found to be non-cytotoxic (IC_{50} > 250). As shown in Figure 2, the cytotoxicity of the ruthenium-glycoside conjugates against HEK293 cells can be ranked in the following order: **3** >> **2** > **4**, which reproduces the tendency found in cancer cell lines. Interestingly, although control complex **1** and aminoglycoside-ruthenium conjugates (**2** and **4**) were more cytotoxic in the normal cell line than in both

cancer cell lines, this tendency was reversed for the guanidinylated conjugate (**3**), which was much less active in HEK293 than in DU-145 cells.

Cell uptake in DU-145 and HEK293 cell lines

To gain insight into the involvement of the glycoside moiety in the cytotoxic activity of the compounds, the cell uptake of the control ruthenium complex (**1**) and of the neomycin-ruthenium (**2**) and guanidinoneomycin-ruthenium (**3**) conjugates was investigated in the prostate cancer cell line and in the normal cell line. Ruthenium accumulation (determined here as the net effect of influx and efflux of Ru) in both cell lines was quantified by inductively-coupled plasma mass spectrometry (ICP-MS)[24,56,57,58] after a 24 h exposure to the compounds at equicytotoxic concentrations, which were in all cases a fifth of their IC_{50} values in each cell line.

As shown in Figure 3, the intracellular level of ruthenium after exposure to neomycin conjugate **2** (107.14 ± 8.93 pmol Ru/10^6 cells) was substantially higher in the DU-145 cell line than guanidinylated analogue **3** (24.10 ± 0.72 pmol Ru/10^6 cells) was, whereas a similar level was obtained in the HEK293 cell line for both compounds (63.75 ± 8.46 pmol Ru/10^6 cells for **2** and 58.02 ± 3.95 pmol Ru/10^6 cells for **3**).

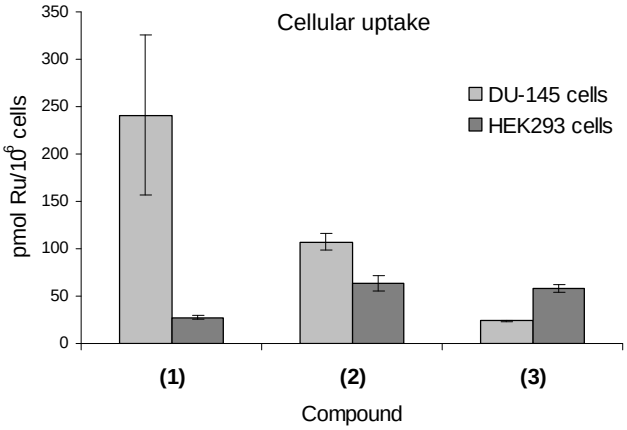

Figure 3. Ruthenium uptake in DU-145 and HEK293 cell lines after 24 h exposure to equicytotoxic concentrations of compounds **1-3**. The ruthenium content is related to the cell number. Results are means of three independent samples and are expressed as mean ± SD.

On the basis of the amount of intracellular ruthenium after exposure to compounds **1-3**, the molar intracellular concentration was calculated by considering the mean cellular

volume, as previously reported by Osella et al.[59] The accumulation ratio was obtained from the ratio between the intracellular concentration and the concentration of the compounds in the extracellular medium at the beginning of the incubation period (IC_{50}/5). As shown in Table 2, the accumulation ratio of the neomycin-ruthenium conjugate (**2**) was similar in both cell lines. However, the accumulation ratio of the guanidinylated analogue (**3**) was much higher than that of **2** both in the cancer DU-145 cell line (about 3-fold) and in the non-tumorigenic HEK293 cell line (about 4-fold). Hence, these results are consistent with the generally accepted idea that the incorporation of guanidinium groups in a molecule facilitates its internalization through cell membrane,[60-62] such as in the case of cell-penetrating peptides. As previously mentioned, cell uptake studies with amino- and guanidinoglycosides had demonstrated an approximately 20-fold internalization enhancement of neomycin upon guanidinylation.[45] In fact, guanidinoneomycin shows similar or even better cell uptake efficiency than some polyarginine-containing peptides,[45,60,61,62] which has been attributed to the semi-rigid pre-organization of the guanidinium groups on the glycoside core.[45] Accordingly, ICP-MS accumulation studies with conjugates **2** and **3** showed the same tendency in both cell lines, since guanidinylation of the neomycin moiety leads to a compound (conjugate **3**) with greater accumulation than its amino precursor (conjugate **2**). Moreover, it should be noted that accumulation of the guanidinylated analogue (**3**) is about 1.4-fold higher in the normal cell than in the tumor cell, whereas **2** is accumulated at the same ratio in both cell lines.

Regarding the parent complex (**1**), as shown in Figure 3, the intracellular level of ruthenium in DU-145 cells (240.86 ± 84.40 pmol Ru/10^6 cells) was much higher than in HEK293 cells (27.64 ± 2.29 pmol Ru/10^6 cells). Similarly, the accumulation ratio was about 3-fold higher in DU-145 than in HEK293 cells (Table 2), which indicates higher accumulation in the prostate cancer cell line than in the normal cell line. In consequence, we can conclude that conjugation of the ruthenium complex through the imidazole ligand to a hydrophilic molecule, either neomycin or guanidinoneomycin, leads to compounds (**2** and **3**) with reduced accumulation in both cell lines, particularly in the case of conjugate **2**, since the incorporation of the guanidinium groups in the glycoside moiety seems to ameliorate this reduction.

Finally, the fact that in all cases the intracellular concentrations were greater than the extracellular concentrations indicates an active cell uptake process for all the compounds, particularly in the case of complex **1** and, to a lesser extent, its guanidinoneomycin conjugate **3**.

	Intracellular concentration (μM)		Accumulation ratio	
Compound / Cell line	DU-145	HEK293	DU-145	HEK293
Ruthenium complex **1**	120.40	13.82	80.29	27.64
Ru-neomycin **2**	53.57	31.87	3.15	3.19
Ru-guanidinoneomycin **3**	12.05	29.01	8.61	12.09

Table 2. Intracellular ruthenium concentrations determined in DU-145 and HEK293 cells after exposure to compounds **1-3** for 24 h at a concentration that was a fifth of their IC_{50} value. The volume of a single cell was considered to be about 2 pL.[63] Accumulation ratio[59] represents the ratio between the intracellular Ru concentration and the Ru concentration in the extracellular medium at the beginning of the incubation period (DU-145: **1**: 1.5 μM, **2**: 17 μM, **3**: 1.4 μM; HEK293: **1**: 0.5 μM, **2**: 10 μM, **3**: 2.4 μM).

DISCUSSION

Current research efforts in metal-based anticancer complexes have focused on the development of new compounds, with the aim of overcoming the high toxicity and sensitivity to resistance of platinum-based drugs in clinical use, such as cisplatin and its analogues.[1-8] Organometallic complexes, in particular ruthenium(II) arene complexes, have attracted attention because of their promising cytotoxic activities in several tumour cell lines, including cisplatin-resistant cells.[6-12] In medicinal chemistry terms, their "piano-stool" structure allows the optimization of lead compounds through structure-activity relationship studies by modifying ligands around the metallic center.[15-16] Among such modifications, derivatization of non-leaving ligands with a carrier molecule has tremendous potential to generate selective, less toxic metallodrugs. The potential of this targeted strategy is particularly promising when metal complexes, either organometallic or classical coordination compounds, are attached to biomolecules[17-24] whose receptors are overexpressed on the membrane of tumoral cells[25-28] or to organic molecules with high affinity with a given biological target

(proteins or nucleic acids).[29] Besides improving selectivity against cancer cells or affinity towards the ultimate target, such modified ligands are also expected to generate hybrid compounds with better pharmacological properties than the original metal complex, such as aqueous solubility or cellular uptake.

This paper reports the effect of conjugating an anticancer ruthenium(II) arene complex (**1**) to amino- and guanidinoglycosides on the cytotoxic activity and cell uptake of the resulting hybrid compounds in cancer and normal cells. The ultimate aim of this project is to develop novel metal-based anticancer compounds with reduced toxicity and side effects that might have RNA as a final biological target. The fact that amino- and guanidinoglycosides are known to be selective RNA binders, might facilitate the interaction of the ruthenium moiety with potential RNA targets involved in the pathogenesis of cancer, such as miRNAs or their precursors (pre-miRNAs). For the synthesis of neomycin- (**2**) and neamine-ruthenium conjugates (**4**), the imidazole ligand incorporated on the suitably-protected aminoglycoside moieties was reacted under microwave irradiation with the complex $[(\eta^6\text{-}p\text{-cym})RuCl(PPh_3)_2]^+$ (Scheme 1). For the guanidinylated analogue of the neomycin conjugate (**3**), the use of *N,N'*-di-Boc-*N''*-triflylguanidine was found compatible with the integrity of the ruthenium moiety. After TFA deprotection, all conjugates were isolated by semipreparative HPLC (overall yields: 45-55%) and fully characterized by high resolution MS and NMR spectroscopy.

The cytotoxicity of conjugates **2-4** together with that of cisplatin, complex **1** and control amino- and guanidinoglycosides was tested in two human cancer cell lines, MCF-7 (breast) and DU-145 (prostate), as well as in a normal cell line, HEK293 (human embryonic kidney). As shown in Table 1, the cytotoxic activity of the ruthenium-glycoside conjugates against cancer and normal cells can be ranked in the following order: **3** >> **2** > **4**. The fact that both natural aminoglycoside antibiotics, neamine and neomycin, and guanidinoneomycin were found to be non-cytotoxic in all cell lines (IC_{50} > 250) indicates that the anticancer activity of compounds **2-4** is provided by the ruthenium moiety. However, an accurate analysis of the IC_{50} values of the compounds reveals that, as well as the ruthenium or the glycoside moieties, the nature of the cell (tumoral or healthy) is another key factor to be considered. Two important observations can be drawn when comparing IC_{50} values of these compounds in the normal cell line with those in cancer cells. On the one hand, ruthenium-aminoglycoside conjugates (**2**

and **4**) were more cytotoxic in the non-tumorigenic cell line than in cancer cells. Effectively, their anti-proliferative activity in HEK293 cells was increased by about two-fold in both cases (e.g. $IC_{50} \approx 80$ μM for conjugate **2** in both cancer cell lines *vs* IC_{50}= 49.4 μM for **2** in the normal cell line). On the other hand, the guanidinylated conjugate **3** was about two-fold less cytotoxic in the healthy cell line than in the DU-145 cell line (e.g. IC_{50} = 12.75 μM *vs* IC_{50} = 7.17 μM, respectively), whereas a similar IC_{50} value was obtained when compared with the MCF-7 cell line (IC_{50} = 11.33 μM), revealing that the response to **3** is also related to the nature of the cancer cells. These results indicate that aminoglycoside-containing conjugates **2** and **4** show the same behavior as their parent ruthenium complex **1**, since their cytotoxicity in normal cells was always greater than in cancer cells. However, this tendency was inverted with the guanidinylated analogue of the neomycin-ruthenium conjugate, since the anti-proliferative activity of **3** in cancer cells was similar to or even higher than in a normal cell line.

Such differences in cytotoxic activity for each compound in a particular cell line, either normal or tumoral, could be interpreted in terms of cell uptake and accumulation efficiency. First, the nature of the aminoglycoside moiety seems to be an important factor, since the cytotoxicity of the neomycin-ruthenium conjugate (**2**) in the three cell lines is about 2.5-fold higher than that of the neamine-containing conjugate (**4**). Although both aminoglycosides are polycations at physiological pH, the greater number of ammonium groups in neomycin than in neamine (six *vs* four) might favor accumulation of conjugate **2**, resulting in a slightly greater antitumoral activity. Second, the fact that the cytotoxicity of the guanidinylated conjugate (compound **3**) in the three cell lines is substantially higher than that of the parent aminoglycoside conjugate (compound **2**) (7-fold in MCF-7 cells, 12-fold in DU-145 cells and 4-fold in HEK293 cells) could be attributed to greater permeability through cell membranes, a property that might facilitate its accumulation in the cell and, for instance, higher anti-proliferative activity. Hence, an apparently good correlation between the expected glycoside uptake efficiency in eukaryotic cells (guanidinoneomycin >> neomycin > neamine) and cytotoxic activity (**3** >> **2** > **4**) can be established in all cell lines, although this does not explain the differences between normal and cancer cells in anti-proliferative activity of the conjugates.

Ruthenium accumulation studies performed by ICP-MS with neomycin (**2**) and guanidinoneomycin (**3**) conjugates in DU-145 and HEK293 cells clearly support the above conclusions. As shown in Table 2, guanidinylation of the aminoglycoside moiety leads to a compound (**3**) with higher accumulation than that of its amino precursor **2**. Indeed, the accumulation ratio of **3** in the cancer cell line was about 3-fold greater than that of **2**, whereas this tendency increased even more in the normal cell line (about 4-fold). These results indicate that guanidinylation of the amino functions at the aminoglycoside moiety in conjugate **2** had a positive effect on cell uptake, thus improving intracellular accumulation. Moreover, it should be noted that the accumulation ratio of conjugate **3** in the normal cell line was 1.4-fold higher than in the cancer cell line, thus revealing behavior the opposite of its amino precursor **2**, which was equally accumulated in both cell lines, or that of control complex **1**, which accumulated at a higher proportion (about 3-fold) in DU-145 than in HEK293.

On the one hand, recent studies have revealed that guanidinoneomycin uptake in CHO cells is mediated by cell-surface heparin-sulfate proteoglycans, which has been used to transport large bioactive cargo into cells at low concentration (nM order) in a selective proteoglycan-dependent manner.[47-49] Thus, we may speculate that differences in the expression level and/or in the composition of proteoglycan receptors on the cell membrane surface between cancer cells and normal cells would be responsible for such differences in the accumulation ratio of **3** between DU-145 and HEK293 cells.[64]

On the other hand, the fact that neomycin- and guanidinoneomycin-ruthenium conjugate's accumulations were lower than that of the parent ruthenium complex **1** also indicates that conjugation to polar, polycationic glycosides results in reduced cell uptake in both cell lines, although this reduction was more dramatic in the cancer cell line. It is well known that lipophilic compounds can cross cell membranes more readily than hydrophilic compounds, which results in increased intracellular accumulation. This is also true for ruthenium(II) arene complexes since an increase in their lipophilicity, for example by increasing the size of the arene ligand, correlates with greater cytotoxicity.[65] Accordingly, the decrease in accumulation of complex **1** when conjugated to neomycin or guanidinoneomycin could be attributed to an overall decrease in the lipophilicity of the compound induced by the highly hydrophilic glycoside moiety, which would

therefore diminish cell uptake. Although the lipophilicity provided by the ruthenium complex (e.g. *p*-cymene and PPh_3 ligands) may modulate the ability of amino(guanidino)glycosides to cross cell membranes when conjugated together, these results seem to indicate that the glycoside moiety, particularly in the case of guanidinoneomycin, has a fundamental weight in the cell uptake of the conjugates.

Overall, on the basis of cytotoxicity and cell uptake studies, in DU-145 cells there is a correlation between accumulation (**1** >> **3** > **2**) and anti-proliferative activity (**1** ≈ **3** >> **2**). The same tendency was found in the case of the normal cell line, since the cytotoxic activity ranking (**1** > **3** >> **2**) follows that of cellular accumulation data (**1** > **3** >> **2**). Interestingly, despite the fact that neomycin-ruthenium conjugate (**2**) accumulation was similar in both cell lines, its anti-proliferative activity was higher in the normal cell than in the tumor cell (about 1.7-fold). An opposite tendency was found for the guanidinylated analogue (**3**), since the cytotoxic activity was higher in the tumor cell line than in the normal cell line (about 1.8-fold), although the accumulation ratio in the normal cell was slightly higher (about 1.4-fold). These results suggest that the glycoside moiety cannot be seen as a simple carrier that modulates the lipophilicity of the anticancer ruthenium(II) arene complex and, for instance, cell uptake, but rather as a dynamic moiety that also modulates the anti-proliferative activity of the metal fragment, depending on the cell type. Indeed, the fact that the anti-proliferative activity of **3** in the DU-145 cancer cells was higher than in the HEK293 normal cells, with a lower accumulation ratio, suggests that guanidinoneomycin provides some kind of selectivity against cancer cells. This hypothesis is supported by the greater cytotoxicity of ruthenium complex **1** or its neomycin conjugate **2** in normal cells than in cancer cells, despite the fact that their accumulation in normal cells is much lower than (**1**) or similar to (**2**) that found in cancer cells. Hence, conjugation to guanidinoneomycin leads to a compound (**3**) with reduced cytotoxicity against normal cells but with a similar anti-proliferative activity to that of the parent ruthenium complex **1** in DU-145 cells.

Finally, we cannot rule out the possibility that amino(guanidino)glycoside conjugation may also modify not only cell uptake in cancer and normal cells, but also the mechanism of action of the ruthenium complex or its biological target. As previously mentioned, guanidinoglycosides have higher binding affinity with RNA sequences than their parent aminoglycosides do. Among aminoglycosides, neomycin derivatives bind

stronger RNA structures than neamine-containing compounds. Hence, given the significant differences in cytotoxicity of the conjugates in both cancer cell lines (IC_{50} ≈ 7-11 μM for **3**, IC_{50} ≈ 80 μM for **2** *vs* IC_{50} ≈ 200 μM for **4**) and in the normal cell line (IC_{50} ≈ 12 μM for **3**, IC_{50} ≈ 50 μM for **2** *vs* IC_{50} ≈ 125 μM for **4**), we may well speculate about the involvement of RNA as a target for these conjugates, since there is close correlation between their anti-proliferative activity (**3** >> **2** > **4**) and the RNA binding affinity of the glycoside moiety (guanidinoneomycin >> neomycin > neamine). The fact that the ruthenium moiety in conjugates **2** and **3** does not follow the typical activation mechanisms of most anticancer organometallic ruthenium complexes (aqueous hydrolysis of the Ru-Cl bond and/or glutathione mediated redox activation) suggests that ruthenation at RNA nucleobases would not occur. However, binding to this biological target could be based on non-covalent interactions such as electrostatic forces and/or hydrogen bonds between the negatively charged skeleton of RNA and the polycationic glycoside moiety. Moreover, aromatic ligands from the ruthenium complex (phenyl rings in PPh_3 and *p*-cymene) could interact with RNA through intercalation or stacking with nucleobases.

In conclusion, the overall results demonstrate the potential of conjugating anticancer metal complexes, in particular organometallic ruthenium(II) complexes, to aminoglycosides, especially to their guanidinylated derivatives, to generate anticancer metal-based drugs with new modes of action. As far as we are aware, such differences between cancer and healthy cells in the cytotoxic activity of amino(guanidino)glycosides conjugated to a ruthenium complex are unprecedented and open the way to the use of guanidinoglycosides to deliver metal-based anticancer agents selectively into tumor cells, with the aim of developing new drugs with reduced toxicity and side-effects. Modifications on the aminoglycoside scaffold, on the metal complex or its properties, or in the number of guanidinium groups might lead to increasing such differences in cytotoxic activity between cancer and normal cells. Moreover, the use of cleavable linkers in the biological media or metal complexes that might be selectively activated (e.g. via irradiation) is expected to improve their potential as anticancer drugs. Since aminoglycosides and their guanidinylated derivatives might be accumulated in some specific cellular compartments such as lysosomes, this strategy would facilitate the detachment of the metallodrug from the glycoside carrier, thus increasing the

effective concentration of the anticancer active species. Further work is in progress to investigate the anticancer activity of these compounds in a wide panel of tumoral cells, as well as to establish their mechanism of action and if RNA is involved as a drug target.

ASSOCIATED CONTENT

Supporting Information

High-resolution ESI MS and NMR spectra of conjugates **2-4** and of intermediates **6** and **9**. Reversed-phase HPLC traces of pure conjugates. This information is available free of charge via the Internet at http://pubs.acs.org.

AUTHOR INFORMATION

Corresponding Author

*Vicente Marchán: Phone +34 934021249, Fax +34933397878, E-mail vmarchan@ub.edu

ACKNOWLEDGEMENTS

This research was supported by funds from Spain's Ministerio de Ciencia e Innovación (grant CTQ2010-21567-C02-01), the Generalitat de Catalunya (2009SGR208), the Instituto de Salud Carlos III (grants RD06/0020/0041) and the Programa d'Intensificació de la Recerca (UB).

REFERENCES

(1) Peacock, A. F. A.; Sadler, P. J. Medicinal organometallic chemistry: Designing metal arene complexes as anticancer agents. *Chem. Asian J.* **2008**, *3*, 1890-1899.

(2) Hartinger, C. G; Dyson, P. J. Bioorganometallic chemistry-from teaching paradigms to medicinal applications. *Chem. Soc. Rev*. **2009**, *38*, 391-401.

(3) Casini, A.; Hartinger, C. G.; Nazarov, A.; Dyson, P. J. Organometallic antitumour agents with alternative modes of action. *Top. Organomet. Chem*. **2010**, *32*, 57-80.

(4) Gasser, G.; Ott, I.; Metzler-Nolte, N. Organometallic anticancer compounds. *J. Med. Chem*. **2011**, *54*, 3-25.

(5) Noffke, A. L.; Habtemariam, A.; Pizarro, A. M.; Sadler, P. J. Designing organometallic compounds for catalysis and therapy. *Chem. Commun*. **2012**, *48*, 5219-5246.

(6) Levina, A.; Mitra, A; Lay, P. A. Recent developments in ruthenium anticancer drugs. *Metallomics* **2009**, *1*, 458-470.

(7) Süss-Fink, G. Arene ruthenium complexes as anticancer agents. *Dalton Trans*. **2010**, *39*, 1673-1688.

(8) Bergamo, A.; Sava, G. Ruthenium anticancer compounds: myths and realities of the emerging metal-based-drugs. *Dalton Trans*. **2011**, *40*, 7817-7823.

(9) Yan, K. Y.; Melchart, M.; Habtemariam, A.; Sadler, P. J. Organometallic chemistry, biology and medicine: ruthenium arene anticancer complexes. *Chem. Commun*. **2005**, *38*, 4764-4776.

(10) Kisova, A.; Zerzankova, L.; Habtemariam, A.; Sadler, P. J.; Brabec, V.; Kasparkova, J. Differences in the Cellular Response and Signaling Pathways between Cisplatin and Monodentate Organometallic Ru(II) Antitumor Complexes Containing a Terphenyl Ligand. *Mol. Pharm*. **2011**, *8*, 949-957.

(11) Allardyce, C. S.; Dyson, P. J.; Ellis, D. J.; Heath, S. L. [Ru(η^6-p-cymene)Cl_2(pta)] (pta = 1,3,5-triaza-7-phosphatricyclo[3.3.1.1]decane): a water soluble compound that exhibits pH dependent DNA binding providing selectivity for diseased cells. *Chem. Commun*. **2001**, *15*, 1396-1397.

(12) Scolaro, C.; Bergamo, A.; Brescacin, L.; Delfino, R.; Cocchietto, M.; Laurenczy, G.; Geldbach, T. J.; Sava, G.; Dyson, P. J. In Vitro and in Vivo Evaluation of Ruthenium(II)-Arene PTA Complexes. *J. Med. Chem*. **2005**, *48*, 4161-4171.

(13) Wang, F.; Chen, H.; Parsons, S.; Oswald, I. D. H.; Davidson, J. E.; Sadler, P. J. Kinetics of aquation and anation of ruthenium(II) arene anticancer complexes, acidity and X-ray structures of aqua adducts. *Chem. Eur. J*. **2003**, *9*, 5810-5820.

(14) Pizarro, A. M.; Habtemariam, A.; Sadler, P. J. Activation mechanisms for organometallic anticancer complexes. *Top. Organomet. Chem*. **2010**, *32*, 21-56.

(15) Jakupec, M. A.; Galanski, M.; Arion, V. B.; Hartinger, C. G.; Keppler, B. K. Antitumor metal compounds: more than theme and variations. *Dalton Trans*. **2008**, *2*, 183-194.

(16) Smith, G. S.; Therrien, B. Targeted and multifunctional arene ruthenium chemotherapeutics. *Dalton Trans*. **2011**, *40*, 10793-10800.

(17) Gross, A.; Metzler-Nolte, N. Synthesis and characterization of a ruthenocenoyl bioconjugate with the cyclic octapeptide octreotate. *J. Organomet. Chem*. **2009**, *694*, 1185-1188.

(18) Metzler-Nolte, N. Biomedical applications of organometal-peptide conjugates. *Top. Organomet. Chem*. **2010**, *32*, 195-217.

(19) Puckett, C. A.; Barton, J. K. Targeting a ruthenium complex to the nucleus with short peptides. *Bioorg. Med. Chem*. **2010**, *18*, 3564-3659.

(20) Splith, K.; Hu, W.; Schatzschneider, U.; Gust, R.; Ott, I.; Onambele, L. A.; Prokop, A.; Neundorf, I. Protease-activatable organometal-peptide bioconjugates with enhanced cytotoxicity on cancer cells. *Bioconjugate Chem*. **2010**, *21*, 1288-1296.

(21) Puckett, C. A.; Barton, J. K. Targeting a ruthenium complex to the nucleus with short peptides. *Bioorg. Med. Chem*. **2010**, *18*, 3564-3659.

(22) Ruiz, J.; Rodríguez, V.; Cutillas, N.; Espinosa, A.; Hannon, M. J. A potent ruthenium(II) antitumor complex bearing a lipophilic levonorgestrel group. *Inorg. Chem.* **2011**, *50*, 9164-9171.

(23) Barragán, F.; López-Senín, P.; Salassa, L.; Betanzos-Lara, S.; Habtemariam, A.; Moreno, V.; Sadler, P. J.; Marchán, V. Photocontrolled DNA binding of a receptor-targeted organometallic ruthenium(II) complex. *J. Am. Chem. Soc*. **2011**, *133*, 14098-14108.

(24) Barragán, F.; Carrion, D.; Gómez-Pinto, I.; González-Cantó, A.; Sadler, P. J.; de Llorens, R.; Moreno, V.; González, C.; Massaguer, A.; Marchán, V. Somatostatin subtype 2 receptor-targeted metal-based anticancer complexes. *Bioconjugate Chem*. **2012**, *23*, 1838-1855.

(25) Mezo, G.; Manea, M. Receptor-mediated tumor targeting based on peptide hormones. *Expert. Opin. Drug. Deliv*. **2010**, *7*, 79-96.

(26) Xia, W.; Low, P. S. Folate-targeted therapies for cancer. *J. Med. Chem*. **2010**, *53*, 6811-6824.

(27) Chen, G. G.; Zeng, Q.; Tse, G. M. K. Estrogen and its receptors in cancer. *Med. Res. Rev.* **2008**, *28*, 954-974.

(28) Ang, W. H.; Dyson, P. J. Classical and non-classical ruthenium-based anticancer drugs: towards targeted chemotherapy. *Eur. J. Inorg. Chem*. **2006**, 4003-4018.

(29) van Zutphen, S.; Reedijk, J. Targeting platinum anti-tumour drugs: Overview of strategies employed to reduce systemic toxicity. *Coord. Chem. Rev*. **2005**, *249*, 2845-2853.

(30) Wang, F.; Xu, J.; Habtemariam, A.; Bella, J.; Sadler, P. J. Competition between Glutathione and Guanine for a Ruthenium(II) Arene Anticancer Complex: Detection of a Sulfenato Intermediate. *J. Am. Chem. Soc*., **2005**, *127*, 17734-17743.

(31) Wu, B.; Ong, M. S.; Groessl, M.; Adhireksan, Z.; Hartinger, C. G.; Dyson, P. J.; Davey, C. A. A Ruthenium Antimetastasis Agent Forms Specific Histone Protein Adducts in the Nucleosome Core. *Chem. Eur. J.* **2011**, *17*, 3562-3566.

(32) Gallego, J.; Varani, G. Targeting RNA with Small-Molecule Drugs: Therapeutic Promise and Chemical Challenges. *Acc. Chem. Res*. **2001**, *34*, 836-843.
(33) Tor, Y. Targeting RNA with small molecules. *ChemBioChem*. **2003**, *4*, 998-1007.
(34) Sharp, P. A. The centrality of RNA. *Cell* **2009**, *136*, 577-580.
(35) Georgianna, W. E.; Young, D. D. Development and utilization of non-coding RNA-small molecule interactions. *Org. Biomol. Chem*., **2011**, *9*, 7969-7978.
(36) Thomas, J. R.; Hergenrother, P. J. Targeting RNA with small molecules. *Chem. Rev*. **2008**, *108*, 1171-1224.
(37) Aboul-da, F. Strategies for the design of RNA-binding small molecules. *Future Med. Chem.* **2010**, *2*, 93-119.
(38) Guan, L.; Disney, M. D. Recent advances in developing small molecules targeting RNA. *ACS Chem. Biol*. **2012**, *7*, 73-86.
(39) Kota, S. K.; Balasubramanian, S. Cancer therapy via modulation of microRNA levels: a promising future. *Drug Discov. Today*, **2010**, *15*, 733-740.
(40) Gandellini, P.; Profumo, V.; Folini, M.; Zaffaroni, N. MicroRNAs as new therapeutic targets and tools in cancer. *Expert Opin. Ther. Targets* **2011**, *15*, 265-279.
(41) Gumireddy, K.; Young, D. D.; Xiong, X.; Hogenesch, J. B.; Huang, Q.; Deiters, A. Small-molecule inhibitors of microRNA miR-21 function. *Angew. Chem. Int. Ed*. **2008**, *47*, 7482-7484.
(42) Deiters, A. Small molecule modifiers of the microRNA and RNA interference pathway. *AAPP J*. **2010**, *12*, 51-60.
(43) Chittapragada, M.; Roberts, S.; Ham, Y. W. Aminoglycosides: molecular insights on the recognition of RNA and aminoglycoside mimics. *Perspect. Med. Chem*. **2009**, *3*, 21-37.
(44) Houghton, J. L.; Green, K. D.; Chen, W.; Garneau-Tsodikova, S. The future of aminoglycosides: the end or renaissance? *ChemBioChem* **2010**, *11*, 880-902.
(45) Luedtke, N. W.; Carmichael, P.; Tor, Y. Cellular Uptake of Aminoglycosides, Guanidinoglycosides, and Poly-arginine. *J. Am. Chem. Soc*. **2003**, *125*, 12374-12375.
(46) Luedtke, N. W.; Baker, T. J.; Goodman, M.; Tor, Y. Guanidinoglycosides: A Novel Family of RNA Ligands. *J. Am. Chem. Soc*. **2000**, *122*, 12035-12036.
(47) Elson-Schwab, L.; Garner, O. B.; Schuksz, M.; Crawford, B. E.; Esko, J. D.; Tor, Y. Guanidinylated neomycin delivers large, bioactive cargo into cells through a heparan sulfate-dependent pathway. *J. Biol. Chem*. **2007**, *282*, 13585-13591.

(48) Sarrazin, S.; Wilson, B.; Sly, W. S.; Tor, Y.; Esko, J. D. Guanidinylated neomycin mediates heparin sulphate-dependent transport of active enzymes to lysozomes. *Mol. Ther.* **2010**, *18*, 1268-1274.

(49) Dix, A. V.; Fischer, L.; Sarrazin, S.; Redgate, C. P. H.; Esko, J. D.; Tor, Y. Cooperative, heparan sulfate-dependent cellular uptake of dimeric guanidinoglycosides. *ChemBioChem* **2010**, *11*, 2302-2310.

(50) Staple, D. W.; Venditti, V.; Niccolai, N.; Elson-Schwab, L.; Tor, Y.; Butcher, S. E. Guanidinoneomycin B recognition of an HIV-1 RNA helix. *ChemBioChem* **2008**, *9*, 93-102.

(51) Boer, J.; Blount, K. F.; Luedtke, N. W.; Elson-Schwab, L.; Tor, Y. RNA-selective modification by a platinum(II) complex conjugated to amino- and guanidinoglycosides. *Angew. Chem. Int. Ed*. **2005**, *44*, 927-932.

(52) Michael, K.; Wang, H.; Tor, Y. Enhanced RNA binding of dimerized aminoglycosides. *Bioorg. Med. Chem*. **1999**, *7*, 1361-1371.

(53) Riguet, E.; Désiré, J.; Bailly, C.; Décout, J-L. A route for preparing new neamine derivatives targeting HIV-1 TAR RNA. *Tetrahedron*, **2004**, *60*, 8053–8064.

(54) Chaplin, A. B.; Dyson, P. J. Catalytic Activity of Bis-phosphine Ruthenium(II)-Arene Compounds: Structure-Activity Correlations. *Organometallics* **2007**, *26*, 2447-2455.

(55) Baker, T. K.; Luedtke, N. W.; Tor, Y.; Goodman, M. Synthesis and anti-HIV activity of guanidinoglycosides. *J. Org. Chem*. **2000**, *65*, 9054-9058.

(56) Egger, A. E.; Rappel, C.; Jakypec, M. A.; Hartinger, C. G.; Heffeter, P.; Keppler, B. K. Development of an experimental protocol for uptake studies of metal compounds in adherent tumor cells. *J. Anal. At. Spectrom*. **2009**, *24*, 51-64.

(57) Groessl, M.; Zava, O.; Dyson, P. J. Cellular uptake and subcellular distribution of ruthenium-based metallodrugs under clinical investigation versus cisplatin. *Metallomics*, **2011**, *3*, 591-599.

(58) Romero-Canelón, I.; Pizarro, A. M.; Habtemariam, A.; Sadler, P. J. Contrasting cellular uptake pathways for chlorido and iodido iminopyridine ruthenium arene anticancer complexes. *Metallomics*, **2012**, *4*, 1271-1279.

(59) Ghezzi, A.; Aceto, M.; Cassino, C.; Gabano, E.; Osella, D. Uptake of antitumor platinum(II)-complexes by cancer cells, assayed by inductively coupled plasma mass spectrometry (ICP-MS). *J. Inorg. Biochem*. **2004**, *98*, 73-78.

(60) Goun, E. A.; Pillow, T. H.; Jones, L. R.; Rothbard, J. B.; Wender, P. A. Molecular transporters: synthesis of oligoguanidinium transporters and their application to drug delivery and real-time imaging. *ChemBioChem*, **2006**, *7*, 1497-1515.

(61) Wender, P. A.; Cooley, C. B.; Geihe, E. I. Beyond cell penetrating peptides: designed molecular transporters. *Drug Discov. Today*. **2012**, *9*, e49-e55.

(62) Lattig-Tunnemann, G.; Prinz, M.; Hoffmann, D.; Behlke, J.; Palm-Apergi, C.; Morano, I,; Herce, H. D.; Cardoso, M. C. Backbone rigidity and static presentation of guanidinium groups increases cellular uptake of arginine-rich cell-penetrating peptides. *Nat. Commun*. **2011**, *2*, 453-458.

(63) Reile, H.; Bernhardt, G.; Koch, M.; Schonenberger, H.; Hollstein, M.; Lux, F. Chemosensitivity of human MCF-7 breast cancer cells to diastereoisomeric diaqua(1,2-diphenylethylenediamine) platinum(II) sulfates and specific platinum accumulation. *Cancer Chemother. Pharmacol*. **1992**, *30*, 113-122.

(64) Bishop, J. R.; Schuksz, M.; Esko, J. D. Heparan sulphate proteoglycans fine-tune mammalian physiology. *Nature*, **2007**, *446*, 1030-1037.

(65) Yan, Y. K.; Melchart, M.; Habtemariam, A.; Sadler, P. J. Organometallic chemistry, biology and medicine: ruthenium arene anticancer complexes. *Chem. Commun*. **2005**, 4764-4776.

Table of Contents Graphic